Monte Carlo study of topological defects in the 3D Heisenberg model

1994 J. Phys. A: Math. Gen. 27 2553

(http://iopscience.iop.org/0305-4470/27/7/030)

J. Phys. A: Math. Gen. 27 (1994) 2553–2563. Printed in the UK

Monte Carlo study of topological defects in the 3D Heisenberg model*

Christian Holm† and Wolfhard Janke‡

† Institut für Theoretische Physik, Freie Universität Berlin, Arnimallee 14, 14195 Berlin, Germany

‡ Institut für Physik, Johannes Gutenberg-Universität Mainz, Staudinger Weg 7, 55099 Mainz, Germany

Received 23 June 1993

Abstract. We use single-cluster Monte Carlo simulations to study the role of topological defects in the three-dimensional classical Heisenberg model on simple cubic lattices of size up to 80^3. By applying reweighting techniques to time series generated in the vicinity of the approximate infinite-volume transition point K_c, we obtain clear evidence that the temperature derivative of the average defect density $\mathrm{d}\langle n\rangle/\mathrm{d}T$ behaves qualitatively like the specific heat, i.e. both observables are finite in the infinite-volume limit. This is in contrast to results by Lau and Dasgupta who extrapolated a divergent behaviour of $\mathrm{d}\langle n\rangle/\mathrm{d}T$ at K_c from simulations on lattices of size up to 16^3. We obtain weak evidence that $\mathrm{d}\langle n\rangle/\mathrm{d}T$ scales with the same critical exponent as the specific heat. As a byproduct of our simulations, we obtain a very accurate estimate for the ratio α/ν of the specific-heat exponent with the correlation-length exponent from a finite-size scaling analysis of the energy.

1. Introduction

It is well known that topological defects can play an important role in phase transitions [1, 2]. Extensively studied examples of systems with point-like defects are the two-dimensional (2D) XY model [3] and defect models for 2D melting [2, 4]. Recently, Lau and Dasgupta (LD) [5] have used Monte Carlo (MC) simulations to study the role of topological defects in the three-dimensional (3D) classical Heisenberg model, where the defects are also point-like objects with a binding energy that increases linearly with the separation [6]. Motivated by the importance of vortex points in the 2D XY model, LD tried to set up a similar pictorial description of the phase transition in the 3D Heisenberg model. Analysing their simulations on simple cubic (SC) lattices of size $V = L^3$, with $L = 8$, 12 and 16, LD claimed that the temperature derivative of the average defect density, $\langle n\rangle$, diverges at the critical temperature T_c like $\mathrm{d}\langle n\rangle/\mathrm{d}T \sim t^{-\psi}$, $t = |T - T_c|/T_c$, with an exponent $\psi \approx 0.65$. They further speculated that $\psi = 1 - \beta$, where $\beta \approx 0.36$ is the critical exponent of the magnetization, and then argued that $\langle n\rangle$ should behave like a 'disorder' parameter.

At first sight, the existence of such a strong divergence of $\mathrm{d}\langle n\rangle/\mathrm{d}T$ seems unlikely, because the definition of defects is quasi-local. It is therefore more likely [7] that $\langle n\rangle$ should behave qualitatively like the energy and $\mathrm{d}\langle n\rangle/\mathrm{d}T$ like the specific heat, which is a finite quantity for the 3D Heisenberg model.

* Work supported in part by Deutsche Forschungsgemeinschaft under grant KI256.

0305-4470/94/072553+11$19.50

Using standard finite-size scaling (FSS) arguments we hence expect to see on finite lattices either

$$\mathrm{d}\langle n\rangle/\mathrm{d}T = L^{\psi/\nu} f(x) \tag{1}$$

or, if the second argument holds true,

$$\mathrm{d}\langle n\rangle/\mathrm{d}T = \text{constant} + L^{\alpha/\nu} g(x) \tag{2}$$

where $\nu \approx 0.7$ and $\alpha \approx -0.1$ are the correlation length and specific heat exponents, respectively, $x = tL^{1/\nu}$ is the FSS variable, and $f(x), g(x)$ are scaling functions. At fixed x, ansatz (1) predicts an approximate linear divergence in L, $\mathrm{d}\langle n\rangle/\mathrm{d}T \sim L^{\psi/\nu} \approx L$. On the other hand, because α is *negative* for the 3D Heisenberg model, ansatz (2) predicts a constant asymptotic value, $\mathrm{d}\langle n\rangle/\mathrm{d}T \sim$ constant. Hence for sufficiently large L a clear distinction between (1) and (2) should be observable.

To decide between the two alternatives we have performed MC simulations on large lattices of size up to $L = 80$, employing the single-cluster update algorithm [8] and reweighting techniques [9]. As a result we find unambiguous support for the second alternative, $\mathrm{d}\langle n\rangle/\mathrm{d}T \sim$ constant, as $L \to \infty$.

As a byproduct of our simulations we numerically extrapolate α/ν from an FSS of the energy in close vicinity of the critical coupling K_c with a much higher accuracy than that obtained in recent high-precision MC studies [10, 11].

2. The simulation

The partition function of the Heisenberg model is given by

$$Z = \prod_i \left[\int \frac{\mathrm{d}\Omega_i}{4\pi} \right] \exp(-KE) \qquad E = \sum_{\langle i,j \rangle} (1 - s_i \cdot s_j) \tag{3}$$

where $K \equiv J/k_B T$ is the (reduced) inverse temperature, s_i are three-dimensional unit vectors at the sites i of an SC lattice, and $\langle i, j \rangle$ denotes nearest-neighbour pairs. Using the single-cluster update algorithm [8] we have simulated the partition function (3) for lattices of size $V = L^3$ with $L = 8, 12, 16, 20, 24, 32, 40, 48, 56, 64, 72, 80$ and periodic boundary conditions. Our main emphasis was on the defect density $n = \sum q^2 n_{|q|}$, where $n_1, n_2, \ldots$ are defect densities of charge $q = \pm 1, \pm 2, \ldots$. To locate these charges we followed the definition of Berg and Lüscher [12], according to which the charge q_{i^*} at the dual lattice site i^* is given by

$$q_{i^*} = \frac{1}{4\pi} \sum_{i=1}^{12} A_i \tag{4}$$

with

$$\cos(\tfrac{1}{2} A_i) = \frac{1 + s_1 \cdot s_2 + s_2 \cdot s_3 + s_3 \cdot s_1}{\sqrt{2(1 + s_1 \cdot s_2)(1 + s_2 \cdot s_3)(1 + s_3 \cdot s_1)}}. \tag{5}$$

The A_i are the directed areas of spherical triangles on the unit 2-sphere with corners s_1, s_2, s_3, whose sign is determined by $\operatorname{sign} A_i = \operatorname{sign}(s_1 \cdot (s_2 \times s_3))$. The spins s_i are

located at the vertices of the cube enclosing the dual site i^*. The four spins at each face of this cube are decomposed into two sets of three spins, giving rise to the twelve A_i in (4). To define a particular decomposition we have introduced the face diagonals running from a site i to $i+e_1+e_2$, $i+e_2+e_3$, and $i+e_3+e_1$, respectively, with e_i, $i=1,2,3$ denoting unit vectors in the three coordinate directions. The spins at the corners of the so-defined triangles are numbered in a counter-clockwise sense relative to the outward pointing normals of the cube enclosing i^*. The decomposition is obviously not unique, but we have checked that other conventions give, on average, the same charges within the error bars. For an SC lattice the distinction between i and i^* is inessential, since the difference is only a uniform translation along the space diagonal.

From the definition of q_{i^*}, it is clear that a trivial upper bound on the magnitude of the lattice topological charge is $q_{i^*} \leqslant 5$. In our runs the highest topological charge observed was three, which occurred on the order of 10^{-7} per site and measurement; see table 1. The likelihood of the appearance of the higher charges was probably too small for them to occur during our run times.

Table 1. Measurement statistics at the simulation point $K_0 = 0.6929$: L is the linear lattice size; N_0 is the number of cluster steps between measurements; N_{meas} is the the number of measurements; τ_n is the integrated autocorrelation time of the charge density; $\langle e \rangle$ is the energy density; $\langle n_{|q|} \rangle$ are the observed densities of dual cells with charge $|q|$ and the total defect density $\langle n \rangle$ is defined as $\langle n \rangle = \langle n_1 \rangle + 4\langle n_2 \rangle + 9\langle n_3 \rangle + \ldots$.

L	N_0	N_{meas}	τ_n	$\langle e \rangle$	$\langle n \rangle \times 10$	$\langle n_1 \rangle \times 10$	$\langle n_2 \rangle \times 10^4$	$\langle n_3 \rangle \times 10^8$
8	17	50178	1.2	1.9487(9)	0.9054(18)	0.88090	6.13	7.78
12	20	159575	1.6	1.9786(3)	0.9845(7)	0.95689	6.90	5.80
16	40	64368	1.2	1.9905(3)	1.0170(9)	0.98838	7.16	7.21
20	50	27670	1.3	1.9968(3)	1.0347(6)	1.0053	7.35	5.42
24	50	20000	1.5	1.9998(2)	1.0431(6)	1.0136	7.38	9.04
32	68	25403	1.5	2.0045(2)	1.0561(4)	1.0260	7.52	6.61
40	74	21765	1.9	2.0063(1)	1.0617(3)	1.0314	7.59	8.04
48	93	21005	1.9	2.0074(1)	1.0646(3)	1.0342	7.61	7.83
56	136	23795	1.6	2.0084(1)	1.0674(2)	1.0369	7.62	6.56
64	200	26439	1.4	2.0090(1)	1.0691(1)	1.0385	7.64	7.18
72	150	20000	1.8	2.0093(1)	1.0701(2)	1.0395	7.65	7.10
80	200	25431	1.7	2.00962(4)	1.0709(1)	1.0403	7.66	6.77

All runs were performed close to the approximate infinite-volume transition point $K_c = 0.6930$, as determined in recent MC studies [10, 11, 13] of this model. Since we wanted to have reference data we performed our simulation at the same coupling, $K_0 = 0.6929$, as in our study of [11] which was close enough to K_c to allow safe reweighting of our data. Because the computation of q_{i^*} is quite complex and thus time consuming, we have performed many cluster update steps between measurements, adjusted in such a way that the (integrated) autocorrelation time of the charge-density measurements is around $\tau_n \approx 1-2$. Since it turned out that the (integrated) autocorrelation times τ_n and τ_χ of the charge density and the magnetic susceptibility were roughly equal, we were able to guess the required measurement interval by extrapolating our previous results for τ_χ [11] to larger lattice sizes L. The measurement statistics are given in table 1. While the statistics are comparable to those in our previous studies [11], and much better than those of LD, we note, that our investigated lattices have much larger linear size up to $L = 80$, compared to $L = 48$ in our previous work, and compared to the largest size $L = 16$ of LD. For each run we recorded the time series of the energy density $e(= E/V)$, the magnetization density $m(= |\sum_i s_i|/V)$

and the charge densities $n_{|q|}$. The resulting averages $\langle e\rangle$, $\langle n\rangle$ and $\langle n_{|q|}\rangle$ can be found in table 1.

To compute the specific heat $C(= \mathrm{d}\langle e\rangle/\mathrm{d}T)$, the thermal expansion coefficient $C_q(= T\mathrm{d}\langle n\rangle/\mathrm{d}T)$ and the topological susceptibility $\chi_q(= \mathrm{d}\langle n\rangle/\mathrm{d}\mu)$, where μ is the 'field' in a fugacity term $\mu\sum_{i^*} q_{i^*}^2$ which one can imagine as adding to the energy in (3) and n is defined as $n = n_1 + 4n_2 + 9n_3 + \ldots$, we used the relations

$$C = VK^2(\langle e^2\rangle - \langle e\rangle^2) = VK^2\langle e;e\rangle \tag{6}$$

$$C_q = VK(\langle en\rangle - \langle e\rangle\langle n\rangle) = VK\langle e;n\rangle \tag{7}$$

$$\chi_q = V(\langle n^2\rangle - \langle n\rangle^2) = V\langle n;n\rangle. \tag{8}$$

To obtain results for the various observables $\mathcal{O}$ at K values in an interval around the simulation point $K_0 = 0.6929$, we applied the reweighting method [9]. Since we recorded the time series this amounts to computing

$$\langle\mathcal{O}\rangle|_K = \frac{\langle\mathcal{O}\mathrm{e}^{-\Delta KE}\rangle|_{K_0}}{\langle\mathrm{e}^{-\Delta KE}\rangle|_{K_0}} \tag{9}$$

with $\Delta K = K - K_0$. To obtain errors we devided each run into 20 blocks and used standard jack-knife errors [14].

Table 2. Results for the matrix elements of the covariance matrix $V\langle O_i;O_j\rangle$, with $O_1 = Ke$ and $O_2 = n$ at $K = 0.6930(\approx K_c)$. Also included are the eigenvalues λ_1, λ_2 of the covariance matrix.

L	C	C_q	χ_q	λ_1	λ_2
8	2.177(18)	0.712(6)	0.369(3)	2.423(19)	0.1225(8)
12	2.407(12)	0.833(5)	0.430(2)	2.721(14)	0.1261(6)
16	2.562(27)	0.908(10)	0.467(4)	2.900(30)	0.1283(9)
20	2.651(36)	0.951(14)	0.486(6)	3.009(40)	0.1277(7)
24	2.752(40)	0.993(17)	0.506(8)	3.128(47)	0.1297(12)
32	2.832(38)	1.027(14)	0.521(6)	3.223(43)	0.1308(12)
40	2.970(45)	1.081(16)	0.542(7)	3.382(51)	0.1300(9)
48	2.977(44)	1.097(18)	0.553(8)	3.400(51)	0.1304(13)
56	3.142(35)	1.157(12)	0.576(5)	3.587(38)	0.1309(13)
64	3.181(30)	1.173(10)	0.579(5)	3.631(33)	0.1286(10)
72	3.142(55)	1.155(19)	0.574(7)	3.585(62)	0.1315(14)
80	3.182(49)	1.169(16)	0.579(6)	3.630(53)	0.1307(12)

The results for the quantities in (6)–(8) at $K_c = 0.6930$ are collected in table 2. Also given are the eigenvalues λ_1, λ_2 of the 2×2 covariance matrix M of e and n with elements $M_{11} = VK^2\langle e;e\rangle$, $M_{12} = M_{21} = VK\langle e;n\rangle$ and $M_{22} = V\langle n;n\rangle$.

3. Results

By applying (9) we have determined the temperature dependence of the quantities in (6)–(8). For small lattices, C_q has its peak location at temperatures larger than T_c, in contrast to C, which peaks at temperature values smaller than T_c. With increasing lattice size, however,

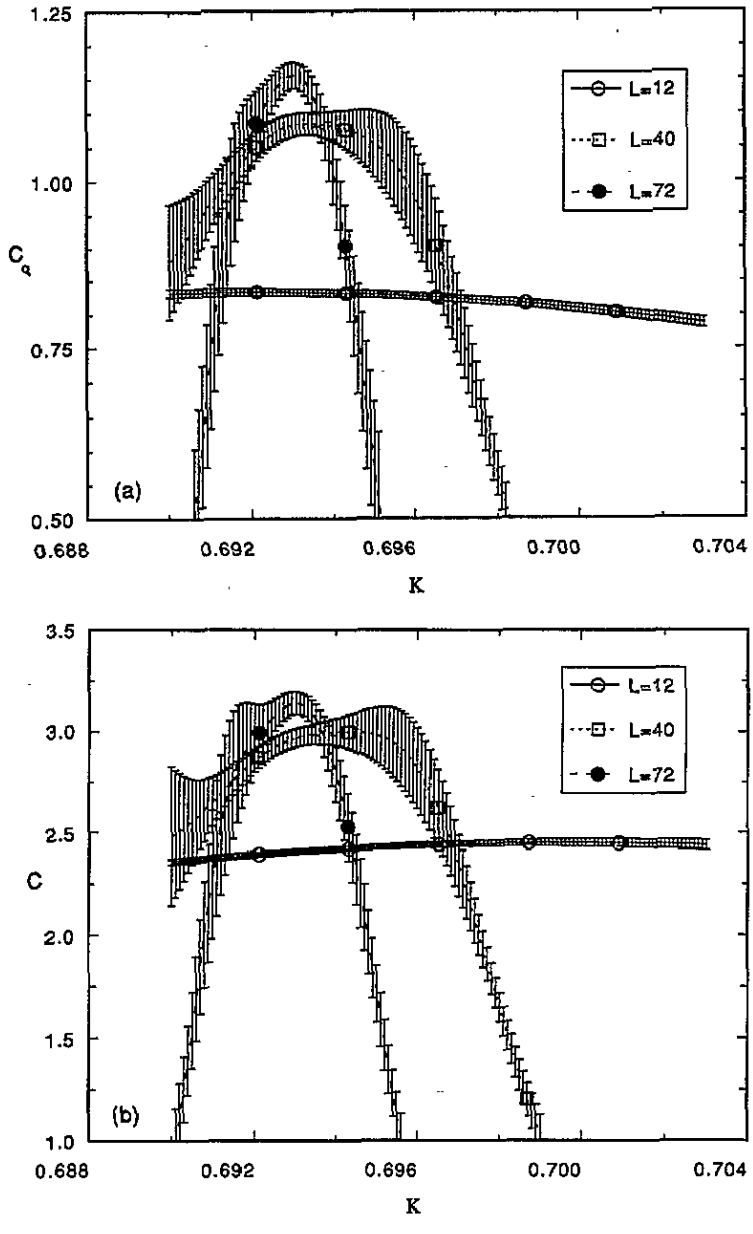

Figure 1. (*a*) $C_q = T\mathrm{d}\langle n\rangle/\mathrm{d}T$ and (*b*) the specific heat C versus K for lattices of size $L = 12$, 40, 72. The values were obtained by reweighting of the runs at $K_0 = 0.6929$.

we observe a strong correlation between C_q and C, that is both quantities develop a smooth peak at roughly the same temperature ($T < T_c$), see figure 1. In contrast to C, the peak locations of C_q scale non-monotonically with a crossover at $L \approx 20$.

We focused first on the scaling behaviour of C_q at our previous estimate of the critical coupling $K_c = 0.6930$, obtained from the crossings of the Binder parameter $U = 1 - \langle m^4\rangle/3\langle m^2\rangle^2$ [11]. Our new data for U on the large lattices confirmed the

constancy of our previous result of $U^* = 0.6217(8)$ and hence our estimate for K_c. We checked first a scaling ansatz for C_q of the form

$$C_q = C_q^{\mathrm{reg}} - a_0 L^{\alpha'/\nu} \tag{10}$$

where C_q^{reg} is a regular background term which is assumed to be independent of lattice size [15]. Note that this ansatz covers both scaling hypotheses (1) and (2). The resulting fit shown in figure 2(a) yields $\alpha'/\nu = -0.401(61)$, $C_q^{\mathrm{reg}} = 1.50(8)$ and $a_0 = 1.82(6)$ with a quality factor $Q = 0.30$ [16]. The good quality of the fit rules out the divergence predicted by ansatz (1) of LD, and strongly favours (2) which predicts a finite asymptotic value for C_q. Only if one assumes that the FSS behaviour sets in at extremely large lattice sizes, could one still attain an assertion of the form (1), but with the consequence of an extremely small exponent ψ. We also tried to reproduce the exponent $\psi \approx 0.65$ of LD by selecting only their lattices sizes and fitting a straight line to our first three data points but even then we obtain a much smaller value of $\psi/\nu \approx 0.36(3)$, leading to $\psi \approx 0.25(3)$. We think that this discrepancy with the result of LD is partly due to our higher statistics and partly due to the fact that we obtained C_q through a thermodynamic derivation, which normally gives better results than the numerical differentiation used by LD.

Because ansatz (2), which was based on the assumption that $\langle n \rangle$ should behave like the energy, fits so well, one can ask whether α' is equal to the specific-heat exponent α. Using our earlier MC result of $\nu = 0.704(6)$ [11], we get a value of $\alpha' = -0.282(46)$, which at first glance, does not strongly support this conjecture. The best field-theoretical estimates are $\nu = 0.705(3)$, $\alpha = -0.115(9)$ and $\alpha/\nu = -0.163(12)$ (resummed perturbation series [17]), while our earlier MC study [11] yielded $\nu = 0.704(6)$, $\alpha = -0.112(18)$ and $\alpha/\nu = -0.159(24)$. However, the accuracy of the values of α is somewhat misleading because they were obtained from hyperscaling, $\alpha = 2 - 3\nu$. The directly measured values have much larger error bars, for example $\alpha/\nu = -0.30(6)$ [10] and $\alpha/\nu = -0.33(22)$ [11].

To compare α' directly with the measured specific-heat exponent of the present MC simulation, we fitted C to

$$C = C^{\mathrm{reg}} - b_0 L^{\alpha/\nu} \tag{11}$$

with a constant background term C^{reg} [15]. The resulting fit in figure 2(*b*) yields $\alpha/\nu = -0.225(80)$, $C^{\mathrm{reg}} = 4.8(7)$ and $b_0 = 4.1(5)$ with $Q = 0.55$ leading to $\alpha = -0.158(59)$. These values are in very good agreement with the hyperscaling prediction, but it is noteworthy that there is a tendency for the values to come out too large.

Of course, a fit of a divergent quantity, like the first derivative $\mathrm{d}C_q/\mathrm{d}T$, for example, is, in principle, numerically much easier to handle. We tried to do this for $\mathrm{d}C_q/\mathrm{d}T$ and $\mathrm{d}C/\mathrm{d}T$ at K_c, and observed the expected divergent scaling behaviour, but unfortunately the statistical errors of the third cumulants involved turned out to be much too large to allow for meaningful fits.

Other estimates for α and α' can be obtained by means of fits of $\langle e \rangle$ and $\langle n \rangle$, which again, qualitatively look very alike. According to (11), we should have, on periodic lattices, a scaling behaviour for the energy density $\langle e \rangle$ of the form [15, 18]

$$\langle e \rangle = \langle e \rangle^{\mathrm{reg}} - d_0 L^{(\alpha-1)/\nu} \tag{12}$$

and because of (10) the topological charge density $\langle n \rangle$ should then accordingly scale like

$$\langle n \rangle = \langle n \rangle^{\mathrm{reg}} - c_0 L^{(\alpha'-1)/\nu}. \tag{13}$$

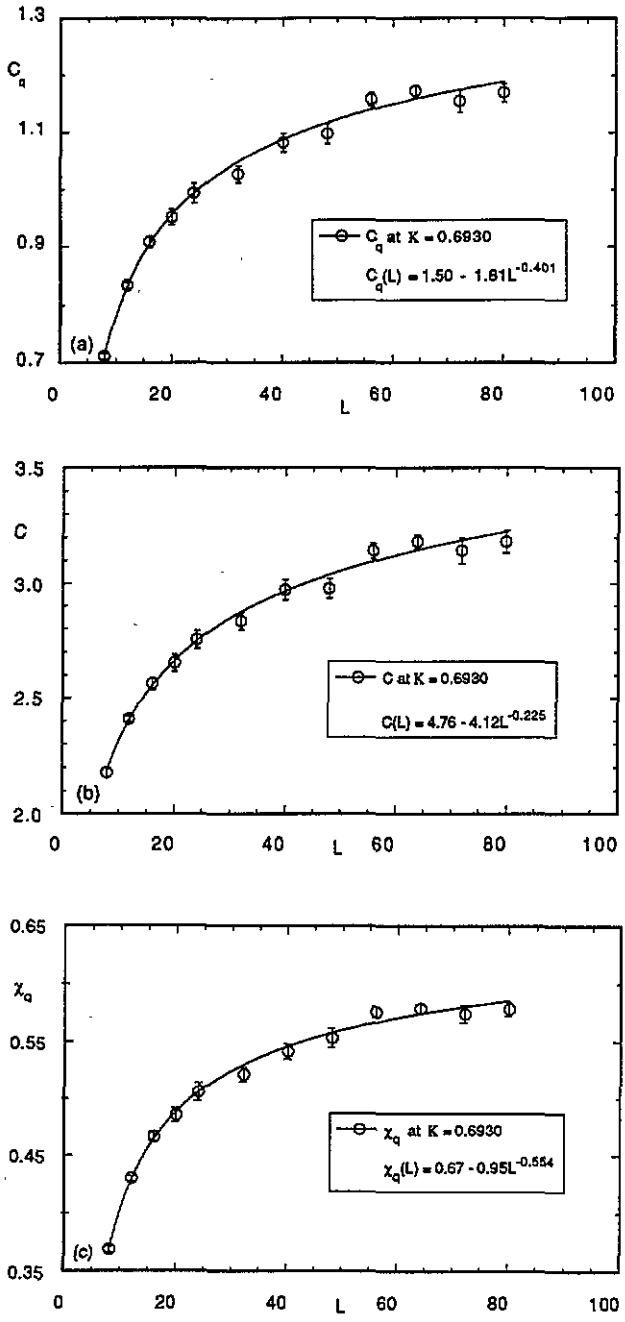

Figure 2. (*a*) C_q, (*b*) C and (*c*) χ_q at $K = 0.6930(\approx K_c)$ as a function of the lattice size L. The full curves show the best nonlinear three-parameter fits to the data.

Fits of these quantities at $K_c = 0.6930$, shown in figure 3, yield $(\alpha' - 1)/\nu = -1.547(15)$, $\langle n \rangle^{\text{reg}} = 0.1074(1)$ and $c_0 = 0.42(2)$, with $Q = 0.30$ and $(\alpha - 1)/\nu = -1.586(19)$, $\langle e \rangle^{\text{reg}} = 2.0106(1)$ and $d_0 = 1.68(8)$, with $Q = 0.25$. This results in $\alpha'/\nu = -0.127(27)$, $\alpha' = -0.089(20)$, $\alpha/\nu = -0.166(31)$ and $\alpha = -0.117(23)$. The results for α and α/ν

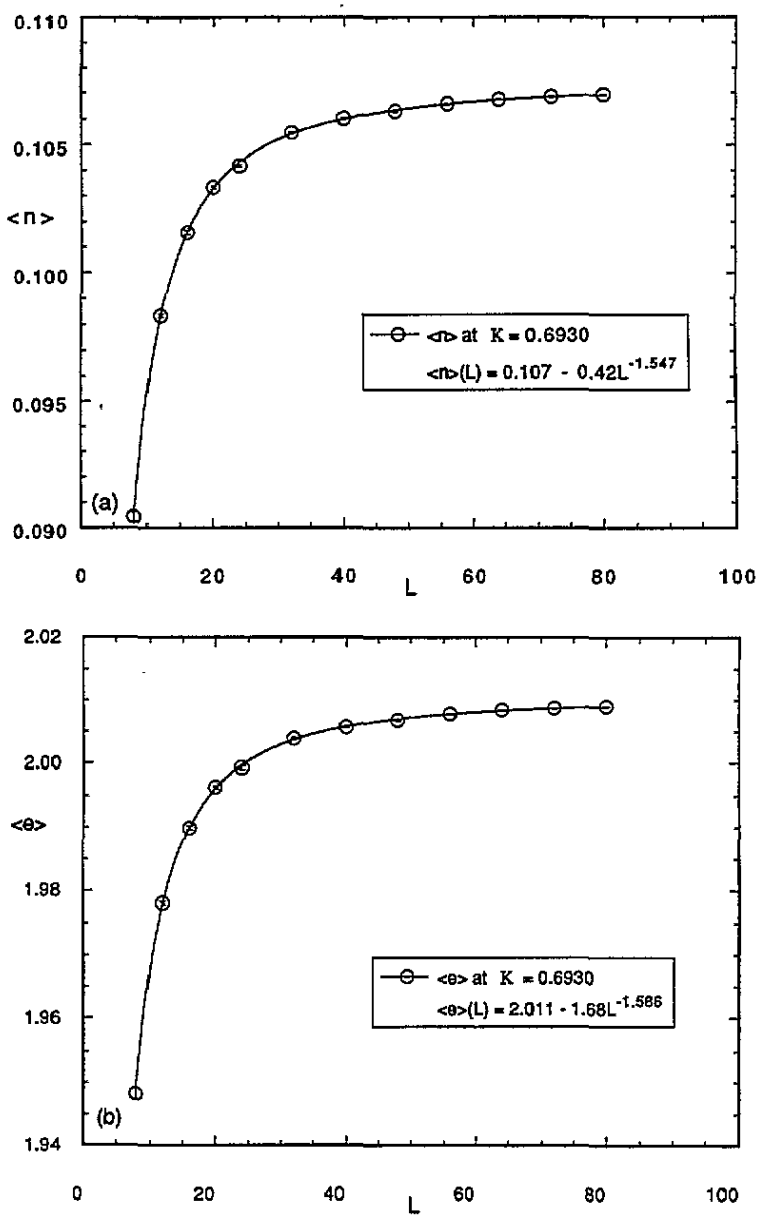

Figure 3. (*a*) $\langle n \rangle$ and (*b*) $\langle e \rangle$ at $K = 0.6930 (\approx K_c)$ as a function of L, together with the best nonlinear three-parameter fits to the data.

are in excellent agreement with the hyperscaling prediction, and have not been directly measured before with such a high precision. We attribute this not only to our large lattice sizes, but also to the fact that we used fits of $\langle e \rangle$ instead of C. The results for α' and α'/ν are now lower than those obtained in (10), but now they are almost consistent with the values for α and α/ν. However, it is still slightly puzzling that both estimates for the exponent α'/ν obtained from the fits (10) and (13) disagree in their respective error range. We attribute this partly to the unknown FSS behaviour of the regular background term $\langle n \rangle^{\text{reg}}$

and partly to the fact that the statistical errors of the three-parameter fits should be taken with great care.

We looked further at the scaling behaviour of χ_q, defined in equation (8). A first look at the plots suggests to try again a scaling ansatz of the form

$$\chi_q = \chi_q^{\text{reg}} - e_0 L^{\alpha''/\nu}. \tag{14}$$

From a three-parameter fit we obtain $\alpha''/\nu = -0.554(57)$, $\chi_q^{\text{reg}} = 0.67(2)$ and $e_0 = 0.95(6)$ with $Q = 0.41$, leading to $\alpha'' = -0.390(44)$. This time it seems already very unlikely that α'' is equal to the specific-heat exponent. However, if one discards the two lowest L values from the fit, one observes a clear trend towards a lower α''-value, but with the drawback of increased error bars and no improvement in χ^2/DOF (per degree of freedom).

We also checked in all our other fits whether there were corrections to the FSS, by discarding successively the data points for $L = 8$ and $L = 12$. We observed in all quantities a trend to the value of α/ν predicted by hyperscaling, but at the price of much larger error bars. Also the χ^2/DOF did not improve. We checked further for confluent corrections [19], by including a term of the form $a_1 L^{-\omega}$, with $\omega = \Delta/\nu$ fixed at the literature value 0.78 [17]. But again the fits were too unstable to give conclusive results.

We also tested whether our results depended strongly on the choice of K_c, by repeating the fits of all quantities at $K_c \pm 0.0002$. The resulting parameters were always consistent with the values at K_c in the one-σ range.

To get a clearer picture we looked further at the scaling behaviour of the eigenvalues of the covariance matrix M of e and n, defined by equations (6)–(8), which give two uncorrelated observables λ_1 and λ_2. Again we used a scaling ansatz of the form

$$\lambda_i = \lambda_i^{\text{reg}} - a_i L^{\alpha_i/\nu}. \tag{15}$$

We obtained $\alpha_1/\nu = -0.273(73)$, $\lambda_1^{\text{reg}} = 5.1(5)$, and $a_1 = 4.7(2)$, with $Q = 0.49$ and $\alpha_2/\nu = -1.45(42)$, $\lambda_2^{\text{reg}} = 0.1307(8)$ and $a_2 = 0.2(2)$, with $Q = 0.60$, leading to $\alpha_1 = -0.192(54)$ and $\alpha_2 = -1.02(31)$. This suggests $\alpha_1 \approx \alpha$ and $\alpha_2 \approx \alpha - 1$. The quality of the fits can be inspected in figure 4.

Because $\lambda_1 + \lambda_2 = C + \chi_q$, then χ_q should scale, at least in part, with an exponent α_2. The existence of an uncorrelated observable which scales with an exponent different from α suggests that we see in our fits of C_q and χ_q corrections to the FSS, a new scaling field or a scaling behaviour with some rationale multiple of α/ν. As long as there is no satisfactory theory for the scaling of topological quantities, however, one cannot decide between these alternatives.

4. Concluding remarks

We have shown that in the three-dimensional classical Heisenberg model the topological defect density $\langle n \rangle$ and its temperature derivative C_q behave qualitatively like the energy $\langle e \rangle$ and its temperature derivative C. In particular, we can reject the conjecture of LD that C_q diverges with a new critical exponent ψ and we find no evidence for an unusual behaviour for the defects near the phase transition.

Rather, our simulations indicate that C_q also behaves quantitatively like the specific heat, i.e. it scales like (2). We obtain weak evidence that, asymptotically for large L, the scaling of C_q is governed by the specific-heat critical exponent α. Still, it cannot be ruled

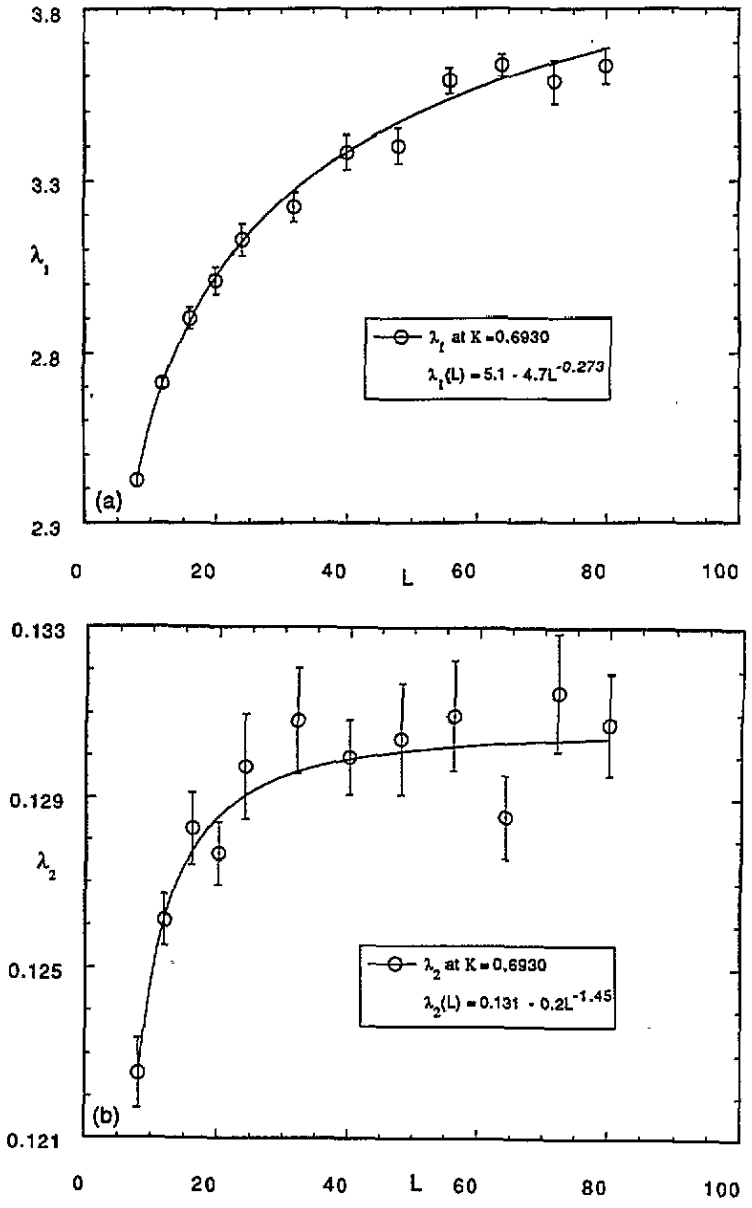

Figure 4. (*a*) λ_1 and (*b*) λ_2 at $K = 0.6930(\approx K_c)$ as a function of L. The best nonlinear three-parameter fits to the data are also included.

out that the scaling of C_q also involves a new exponent belonging to a new scaling field. For the topological susceptibility χ_q, we find that it also remains finite, and that it can be fitted with an ansatz of the form (2) as well, but that its scaling exponent deviates from α. Our fits of the eigenvalues λ_i of the covariance matrix seem to indicate that C_q and χ_q are a mixture of a part which scales with α and a part which scales according to $\alpha - 1$.

Finally, the present fits of the specific heat at K_c yielded a value of α of better accuracy and in better agreement with the hyperscaling value than fits of the specific-heat maxima

as used in previous works [10, 11], which we attribute to our large lattice sizes, the larger number of available data points, and to the fact, that our data and fit were performed extremely close to the critical temperature. Moreover, by fitting the *energy* at K_c to equation (12), we obtained an estimate for α/ν with a precision unprecedented by direct numerical MC simulations and in accuracy comparable to hyperscaling predictions.

Acknowledgments

We are indepted to AD Sokal for discussions that initiated this study. WJ thanks the DFG for a Heisenberg fellowship. The numerical simulations were performed on the CRAY X-MP and Y-MP at the Konrad-Zuse Zentrum für Informationstechnik Berlin (ZIB), and the CRAY X-MP at the Rechenzentrum der Universität Kiel. We thank all institutions for their generous support.

References

[1] Halperin B I 1980 *Physics of Defects (Proc. Les Houches Summer Institute)* (Amsterdam: North-Holland)
[2] Kleinert H 1989 *Gauge Fields in Condensed Matter* (Singapore: World Scientific)
[3] Berezinskii V L 1971 *Zh. Eksp. Teor. Fiz.* **61** 1144; 1972 *Sov. Phys. –JETP* **34** 610
Kosterlitz J M and Thouless D J 1973 *J. Phys. C: Solid State Phys.* **6** 1181
Kosterlitz J M 1974 *J. Phys. C: Solid State Phys.* 7 1046
[4] Nelson D R and Halperin B I 1979 *Phys. Rev.* B **19** 2457
Strandburg K J 1988 *Rev. Mod. Phys.* **60** 161 and Erratum 1989 **61** 747
Janke W 1990 *Int. J. Theoret. Phys.* **29** 1251
[5] Lau M-H and Dasgupta C 1988 *J. Phys. A: Math. Gen.* **21** L51; 1989 *Phys. Rev.* B **39** 7212
[6] Ostlund S 1981 *Phys. Rev.* B **24** 485
[7] Sokal A D 1992 private communication
[8] Wolff U 1989 *Phys. Rev. Lett.* **62** 361
[9] Ferrenberg A M and Swendsen R H 1988 *Phys. Rev. Lett.* **61** 2635 and Erratum 1989 **63** 1658
[10] Peczak P, Ferrenberg A M and Landau D P 1991 *Phys. Rev.* B **43** 6087
[11] Holm C and Janke W 1993 *Phys. Lett.* **173A** 8; 1993 *Phys. Rev.* B **48** 936; 1993 *Nucl. Phys.* B (Proc. Suppl.) **30** 846
[12] Berg B and Lüscher M 1981 *Nucl. Phys.* B **190** [FS3] 412
[13] Chen K, Ferrenberg A M and Landau D P 1993 *Preprint* UGA
[14] Miller R G 1974 *Biometrika* **61** 1
Efron B 1982 *The Jackknife, the Bootstrap and other Resampling Plans* (Philadelphia, PA: SIAM)
[15] Privman V (ed) 1990 *Finite-Size Scaling and Numerical Simulations of Statistical Systems* (Singapore: World Scientific) p 4
[16] Press W H, Flannery B P, Teukolsky S A and Vetterling W T 1986 *Numerical Recipes—The Art of Scientific Computing* (Cambridge: Cambridge University Press)
[17] Le Guillou J C and Zinn-Justin J 1980 *Phys. Rev.* B **21** 3976
[18] For a numerical MC test of the free energy behaviour of the three-dimensional Ising model see:
Mon K K 1985 *Phys. Rev. Lett.* **54** 2671; 1989 *Phys. Rev.* B **39** 467
[19] Wegner F J 1972 *Phys. Rev.* B **5** 4529